IR BANDSHAPES OF WEAKLY H-BONDED SYSTEMS. I. COMPLEXES OF TRIPHENYLCARBINOL AND TRIMETHYLCARBINOL

By J. P. Hawranek and T. Gostyńska

Institute of Chemistry, University of Wrocław**

(Received November 28, 1979)

IR spectra of Triphenylcarbinol and Trimethylcarbinol in a series of solvents of increasing proton acceptor ability were measured. A detailed analysis of shape of the stretching vibration band of the proton donor group in these systems was carried out. The shape of the band was characterized in terms of profile indices, band moments, asymmetry factors, correlation functions and correlation times. The role of various shaping mechanisms is discussed in the framework of recent theories of IR spectra of weakly H-bonded systems.

1. Introduction

The evolution of the shape of the stretching vibration band of the proton-donor group AH, involved in a hydrogen bond R′AH···BR″ is qualitatively well known. With increasing strength of the interaction the ν_s(AH) band is being progressively shifted to lower frequencies and considerably broadened. For weak H-bonds the contour remains smooth, but starting from a certain strength of the bridge the smooth shape is disturbed by appearance of structure.

Several advanced theories have been presented recently, elucidating factors contributing to the broadening of the band and attempting a quantitative description of the profile of the ν_s(AH) band for weak and medium strength H-bonded systems [1–9]. Substantial progress has been made in the understanding of mechanisms responsible for the shaping of these bands in H-bonded complexes in solution. Janoschek, Weidemann and Zundel [3, 4], Rösch and Ratner [7] hold responsible for the broadening the coupling of the fluctuating local electric field set up by the internal modes of the "bath" surrounding

* This work was supported by the Polish Academy of Sciences under the MR.I.-9 plan.

** Address: Instytut Chemii, Uniwersytet Wrocławski, F. Joliot-Curie 14, 50-383 Wrocław, Poland.

the complex, with the dipole moment of the complex. Bratos [8] presented a theory invoking the direct coupling between ν_s(AH) and ν_σ(AH···B). Robertson and Yarwood [9], basing on the same idea, presented a model of vibrational relaxation in H-bonded systems, according to which the ν_s(AH) mode is loosing phase coherence through this coupling because of the energetic contact of the ν_σ mode with the brownian motion of the solvent molecules; strong experimental support for this mechanism was given [10]. De Bleijser and all [11, 12] pointed out the possibility of a further broadening mechanism in H-bonded systems, resulting from vibrational relaxation by near-resonant vibrational energy transfer to solvent molecule modes. The effect of electrical anharmonicity was shown to be of weak spectral activity [13]. Some role in the blurring of the details of the fine structure of the band could be played by dissociative relaxation [14]. Finally, the possibility of a reorientational contribution to the overall broadening, although anticipated to be small, should not be a priori discarded [14–18].

Despite substantial theoretical progress, quantitative experimental data on profiles and intensities of H-bonded species in solution are still scarce. This does not facilitate the discussion of the role of various factors influencing the profile. The scarcity of experimental data is probably caused by experimental and numerical difficulties encountered with the measurement and analysis of shape in quantitative terms.

The aim of this work is to obtain systematic data on band profiles in weak H-bonded systems, with the hope that such studies may help to elucidate and disentangle the various dynamic phenomena occurring in the complex.

It is not easy to select H-bonded systems suitable for quantitative bandshape studies. They have to meet all conditions for the demonstration of the pure effect of H-bond formation on the profile of the IR bands of the R′AH···BR″ complex. Commonly encountered experimental difficulties are: (*i*) self association of the donor R′AH, forming e.g. dimers $(R'AH)_2$; (*ii*) formation of several complexes of various stoichiometry, e.g. R′AH···BR″ and $(R'AH)_2BR''$, (*iii*) not complete bonding of the donor, causing free R′AH and bonded R′AH···BR″ donor molecules to coexist in solution. All these factors give rise to less or more overlapping bands, thus masquing the "pure" effect of H-bond formation on the shape of the ν_s band. Other interfering effects, such as averlap with other vibrations of the donor, acceptor (and solvent, if studied in three-component systems), hot bands, Fermi resonances and isotopic splittings may also obscure the bandshape. Finally, traces of water, which is strongly absorbing in the same region as all OH-type donors, can affect the results.

Additionally, instrumental factors causing band broadening and bandshape distortion have to be avoided by careful choice of scanning parameters or removed by numerical correction procedures [19, 20]. Fortunately, because of the considerable breadth of the ν_s band in H-bonded systems, the problem is less critical here than with common vibrational bands.

In this work, Triphenylcarbinol (TPC) and Trimethylcarbinol (TMC) were selected as donors. TPC is especially suitable for this purpose, as it does not self-associate at low concentrations and it is not hygroscopic. TMC is more difficult to handle in this respect. As acceptors, a series of solvents of increasing basicity was chosen.

2. Experimental

The IR spectra were recorded on a Perkin–Elmer Model 180 IR Spectrophotometer. The scan speed was ca. 5 cm^{-1}/min, with a time constant of 1.5 sec; this conditions were sufficient to avoid any mechanical or electronic distortion of the measured bandshapes [19, 20]. The spectral slit width was maintained constant and set in the limits 1–2 cm^{-1}. This ensured that the ratio of the spectral slit width to the apparent half-width of the band, $\frac{s}{(\Delta\nu_{1/2})^a}$ was maintained below 0.1, thus excluding any optical distortion of the profile [19, 20], so no deconvolution was needed.

Good commercial grade solvents were purified and dried following standard methods [21] and stored over molecular sieves or sodium (where applicable). The spectral measurements were carried out in NaCl and KBr cells, at 300 K, following the compensation technique, i.e. using a matched pair of cells, with the pure solvent placed in the reference beam. "Drawn-in" baselines were used, obtained by joining the flat ends of the recorded transmission spectrum with a straight line. The problems with the choice of an appropriate procedure for determining the baseline are well known [10]. It should be mentioned, that there is no straightforward solution of the baseline problem, as in principle, there can be no exact baseline determination in the transmission spectrum, because of the reflection losses, which differ on both sides of the band because of the anomalous dispersion of the refractive index in the region of absorption [22]. In practice one can minimize the error by measuring several samples and averaging the results. The spectra were subsequently digitized and processed in the Computation Centre of the University of Wrocław. The shape of the bands was analyzed on three independent ways.

3. Numerical analysis of shape

3.1. Band fitting

Each experimental scan of the band was fitted by means of an asymmetric Cauchy–Gauss product bandshape function [23] in an iterational process

$$A_l(\nu) = a_1[1+a_2^2(\nu-a_3)^2]^{-1}\exp[-a_4^2(\nu-a_3)^2] \quad \text{for} \quad \nu \geqslant a_3,$$

$$A_r(\nu) = a_1[1+a_5^2(\nu-a_3)^2]^{-1}\exp[-a_6^2(\nu-a_3)^2] \quad \text{for} \quad \nu < a_3, \tag{1}$$

$A_l(\nu)$ and $A_r(\nu)$ approximate the experimental absorbance curve $\lg_{10}\left(\frac{I_0}{I}\right)_\nu$ at the "left" (high frequency) and "right" (low frequency) side of the band, respectively; ν denotes wavenumber [cm^{-1}], a_3 is the band maximum position ν_m, a_1 stands for the peak height (in decadic absorbance units) and a_2, a_4, a_5, a_6 are shape parameters. All six parameters a_1, a_2, a_3, a_4, a_5, a_6 are treated as adjustable and are obtained simultaneously in the iterational process. The use of this flexible analytical function allows to describe the shape and analyze the asymmetry of the band with high precision [23]; it must be emphasized, however, that the description is purely empirical and it is carried out only to smooth the curve and

to facilitate further data processing. The bandshape parameters lack a direct interpretative view (apart from a_1 and a_3), but several useful secondary quantities can be calculated, characterising the profile, e.g. arbitrary profile indices $L_l = \frac{a_2}{a_2+a_4}$, $L_r = \frac{a_5}{a_5+a_6}$, giving the Lorentz contribution to the profile; b_l and b_r — the widths of the left and right parts of the band at half-height (the total half width of the band is b_l+b_r). The integrated intensities of the low and high frequency parts of the band are given by:

$$B_r = \frac{1}{c \cdot l} \int_0^{\nu_m} A_r(\nu) d\nu, \tag{2}$$

$$B_l = \frac{1}{c \cdot l} \int_{\nu_m}^{\infty} A_l(\nu) d\nu, \tag{2'}$$

and the total absolute intensity of the band is $B = B_l + B_r$, where l denotes pathlength expressed in [cm] and c is concentration; if c is expressed in [mole l^{-1}], the intensity is obtained in the IUPAC practical unit [19] [$l \cdot \text{mole}^{-1}\,\text{cm}^{-2}$], which corresponds to [10^3 cm mole^{-1}]. The asymmetry of the band can be very conveniently characterized by the ratio of the integrated intensities of the low and high frequency side of the band

$$k_a = \frac{B_r}{B_l}. \tag{3}$$

3.2. Central moments

To analyze separately the shape of the low- and high-frequency side of the band, the second and fourth truncated central band moments [19, 20] were calculated, according to the formula given here only for the high frequency side

$$\mu_{n,l}(j) = \frac{1}{b_l^n} \frac{\int_{-j}^{j} (\nu - \nu_m) A_l(\nu) d\nu}{\int_{-j}^{j} A_l(\nu) d\nu}, \tag{4}$$

where $n = 2, 4$ and $j = \frac{\nu - \nu_m}{b_l}$. The truncated band moments provide a tool to characterize the shape via the β_l and β_r parameters defined as:

$$\beta_l = \frac{\mu_{4,l}}{\mu_{2,l}^2}; \quad \beta_r = \frac{\mu_{4,r}}{\mu_{2,r}^2}. \tag{5,5'}$$

For a pure Gauss curve, $\beta = 3$; for a curve with "mixed" shape, $\beta > 3$ [19].

It should be noted here, that more precisely $\mu_{n,l}(j)$ and $\mu_{n,r}(j)$, calculated from Eq. (4), represent central truncated moments of "artificial" symmetrical bands, assembled from two "left" and two "right" parts of the real asymmetrical bands, respectively.

3.3. Correlation functions

Correlation functions were calculated from the formula

$$G(t) = \frac{\int_0^\infty S(\nu) \cos [2\pi c(\nu - \nu_m)t] d\nu}{\int_0^\infty S(\nu) d\nu}, \tag{6}$$

where $S(\nu)$ is the experimental spectral density function [24]. The correlation functions were recalculated with respect to the shifted band origin, i.e. the first initial moment of the band, which reflects also the asymmetry of the band:

$$\nu_0 = \frac{\int_0^\infty \nu S(\nu) d\nu}{\int_0^\infty S(\nu) d\nu}. \tag{7}$$

The differences were found negligible, except for strongly asymmetric bands [24]. The correlation time t_c was estimated by numerical integration of the correlation function

$$t_c = \int_0^\infty G(t) dt. \tag{8}$$

4. Results and discussion

4.1. Band contours and asymmetry

The contours of the ν_s(OH) absorption bands, studied in two-component systems, reproduced from averaged experimental data (5–6 scans), are presented in Fig. 1 for TPC and Fig. 2 for TMC. The spectral data are collected in Table I for TPC and in Table II for TMC.

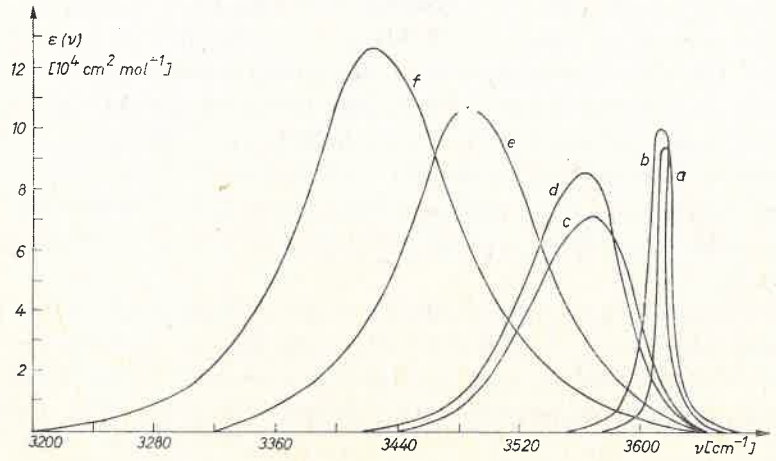

Fig. 1. Contours of the ν_s(OH) band of Triphenylcarbinol in: *a* — Heptane, *b* — Carbon Tetrachloride, *c* — Nitrobenzene, *d* — Nitromethane, *e* — Acetonitrile, *f* — Dioxane

As can be seen from Table I, the ν_s(OH) band of TPC exhibits a distinct asymmetry in inert solvents (heptane, CCl_4), which is especially pronounced in CCl_4. The spectral data for this band in heptane, as well as for TMC in heptane are close to those reported by Kirchner and Richter [29] for decane d-22. Our data for TMC in CCl_4 agree well with those of Lutz and Der Maas [30], except, that we find $\frac{b_l}{b_r} = 0.9$. The asymmetry of this band is however much less pronounced than for TPC.

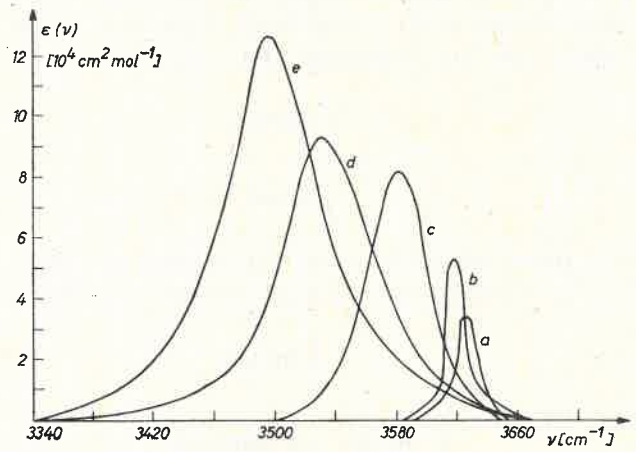

Fig. 2. Contours of the ν_s(OH) band of Trimethylcarbinol in: *a* — Heptane, *b* — Carbon Tetrachloride, *c* — Nitrobenzene, *d* — Acetonitrile, *e* — Dioxane

From Figs 1 and 2, and from the data of Tables I and II typical IR-features, accompanying the formation of weak H-bonds can be observed: decrease of the position of the maximum of the band, ν_m; increase of total bandwidth, $b_l + b_r$; increase of absolute intensity, B. The absolute intensity was calculated from Eqs. (2), (2′) with the assumption, that the total amount of the donor R′AH exists in solution in the complex form R′AH···BR″. This assumption does not raise any doubts as only a single band is observed in the studied wavenumber range, corresponding to the bonded AH···B oscillator, and no "free" AH band is observed. This does not hold, however, in the case of π-complexes with benzene and mesitylene, as will be discussed later in this chapter. The spectra were measured at relatively low concentrations of the donors (0.01–0.06 mole dm^{-3} for TPC, 0.01–0.05 mole dm^{-3} for TMC), so possible disturbing selfassociation effects were entirely eliminated [25].

Whereas in inert and slightly active solvents the low frequency side of the ν_s(OH) band is more intense ($k_a < 1$, $\nu_0 < \nu_m$), for stronger interactions an inversion of the intensity occurs; for acetonitrile and dioxane the high frequency side is more intense (Table I, Table II). This can be probably explained by the inversion of sign of electrical anharmonicity [13].

An interesting feature is emerging from the typical picture seen in Fig. 1 and Fig. 2: whereas for TPC complexes ε_{max} does not change considerably with increasing strength

TABLE I

Results of numerical bandshape analysis for the ν_s(OH) band of Triphenylcarbinol. Errors quoted are root mean square errors of the arithmetic mean

Parameter \ Solvent		Heptane	Carbon Tetrachloride	Nitrobenzene	Nitromethane	Mesitylene[a]		Acetonitrile	Dioxane
ν_m	[cm^{-1}]	3617.1 ±0.2	3612.2 ±0.1	3571.1 ±1.3	3563.0 ±0.8	3559.9 ±0.2	3613.0±0.5	3485.8 ±0.2	3424.0 ±0.1
ν_0	[cm^{-1}]	3616.6	3608.2	3555.8	3550.2	3563.1		3486.7	3430.3
ε_{max}	[$10^4 cm^2 mole^{-1}$]	9.73±0.26	10.02±0.09	7.18±0.09	8.62±0.18	7.39±0.03		10.79±0.14	12.66±0.06
b_l	[cm^{-1}]	5.3 ±0.2	6.1 ±0.1	29.2 ±0.9	30.1 ±0.4	22.9 ±0.3	9.1±0.5	56.9 ±1.3	63.6 ±0.7
b_r	[cm^{-1}]	6.1 ±0.1	8.8 ±0.0	50.1 ±1.3	44.1 ±0.8	20.4± 0.3	9.1±0.5	48.2 ±0.1	55.1 ±0.2
b_l+b_r	[cm^{-1}]	11.4 ±0.2	14.9 ±0.1	79.4 ±0.4	74.2 ±0.8	43.4 ±0.1	18.2±1.0	105.1 ±1.4	118.7 ±0.7
L_l°	[%]	87.9 ±1.8	86.0 ±0.5	7.0 ±3.3	25.2 ±1.8	75.1 ±0.9	76.6±0.4	60.0 ±0.3	67.5±2.7
L_r	[%]	83.0 ±1.5	89.0 ±0.7	38.8 ±5.4	59.2 ±2.4	71.5 ±1.4	76.6±0.4	75.4 ±0.5	69.5±0.2
β_{2l}		8.3 ±0.6	7.6 ±0.2	3.00±0.00	3.02±0.01	4.9 ±0.1	5.2±0.1	3.7 ±0.1	4.2±0.2
β_{2r}		6.7 ±0.5	8.7 ±0.2	3.17±0.07	3.68±0.11	4.5 ±0.1	5.2±0.1	5.0 ±0.1	4.3±0.02
B_l	[$10^6 cm \cdot mole^{-1}$]	0.745±0.026	0.832±0.012	2.23±0.06	2.77±0.09	2.05±0.02		6.97±0.25	9.48±0.50
B_r	[$10^6 cm \cdot mole^{-1}$]	0.800±0.011	1.223±0.017	3.89±0.11	4.30±0.11	1.81±0.01		6.43±0.08	8.29±0.03
B	[$10^6 cm \cdot mole^{-1}$]	1.545±0.037	2.055±0.018	6.12±0.09	7.07±0.19	3.86±0.02		13.40±0.32	17.77±0.52
k_a		1.08 ±0.01	1.46 ±0.02	1.75±0.09	1.56±0.03	0.88±0.01		0.93±0.02	0.87±0.02

[a] Value of ε_{max}, B_l, B_r and B quoted for Mesithylene are only approximate, as the equilibrium constant between the two forms is unknown.

TABLE II

Results of numerical bandshape analysis for the ν_s(OH) band of Trimethylcarbinol

Parameter \ Solvent		Heptane	Carbon Tetrachloride	Nitrobenzene	Acetonitrile	Dioxane
ν_m	[cm^{-1}]	3623.6 ±0.5	3618.1 ±0.1	3580.9 ±0.5	3530.9 ±0.1	3494.3 ±0.4
ν_0	[cm^{-1}]	3623.8	3618.0	3579.0	3528.7	3503.4
ε_{max}	[10^{4}cm^{2}mole^{-1}]	3.60±0.04	5.69±0.11	7.89±0.02	9.33±0.08	12.62±0.95
b_l	[cm^{-1}]	7.6 ±0.1	6.8±0.1	24.7 ±0.5	40.1 ±0.3	40.8 ±0.4
b_r	[cm^{-1}]	8.2 ±0.1	7.7 ±0.1	24.1 ±1.0	32.0 ±0.9	34.8 ±0.3
b_l+b_r	[cm^{-1}]	15.8 ±0.1	14.5 ±0.1	48.8 ±0.5	72.1± 1.2	75.6 ±0.1
L_l	[%]	84.2 ±0.3	83.0 ±0.9	7.3 ±3.0	72.9 ±0.6	83.5 ±1.4
L_r	[%]	77.9 ±0.5	76.6 ±0.7	62.8 ±2.0	87.6 ±0.8	80.0 ±0.2
β_{2l}		6.9 ±0.1	6.6 ±0.3	3.00±0.00	4.7 ±0.1	6.8 ±0.4
β_{2r}		5.4 ±0.1	5.2 ±0.1	3.8 ±0.1	8.2 ±0.3	5.8 ±0.1
B_l	[10^{6}cm · mole^{-1}]	0.360±0.014	0.501±0.006	2.05±0.05	4.61±0.05	6.81±0.05
B_r	[10^{6}cm · mole^{-1}]	0.374±0.007	0.543±0.007	2.22±0.12	4.31±0.03	5.63±0.06
B	[10^{6}cm · mole^{-1}]	0.734±0.020	1.035±0.015	4.27±0.08	8.92±0.08	12.44±0.04
k_a		1.03±0.01	1.06±0.01	1.06±0.06	0.94±0.01	0.83±0.01

of the H-bond (Fig. 1) and the total intensity increase can be correspondingly attributed to the broadening mechanism, this is not the case for TMC complexes (Fig. 2), for which a serious increase of ε_{max} occurs. This is in contradiction to the findings of the fluctuating field broadening theory, according to which the "bath" should broaden, but not intensify the ν_s(AH) band of the complex in solution [7].

The numerical fitting of the experimental band shape with the asymmetric Cauchy--Gauss product function enabled us to approximate the bands routinely with an average mean deviation smaller than 0.002 absorbance units (in decadic logarithms). The profile indices and central moments for the ν_s(OH) bands of both Triphenylcarbinol and Trimethylcarbinol in inert solvents (Heptane and CCl_4) indicate, that the shape deviates distinctly from pure Lorentzian curves, in contradiction to the findings of other Authors [29]. This is probably due to the assumption of a symmetric profile in those studies [29], whereas, as was discussed before, the ν_s(OH) band — especially of TPC — shows a distinct and appreciable asymmetry in inert solvents.

The profile indices of both sides of the band do not differ considerably, except for nitrobenzene and nitromethane. It can be noticed, however, that with increasing strength of the H-bond interaction the gaussian component increases — in both sides of the band; this trend is observed for both studied series. An increase of the Gauss component with

H-bond formation was observed also by Kirchner and Richter [29] for several intramolecularly H-bonded phenyl-substituted alcohols. The lorentzian contribution remains however still very considerable; this is reflected in the β_l and β_r parameters, which are considerably greater than 3 in majority of cases, as well as in the profile indices L_l and L_r (Table I, Table II). These findings can be compared with the results of Bratos theory [8, 13] which predicts the ν_s(AH) bandshape of a weak complex to be an asymmetrically distorted gaussian; it is not possible to go too far with the comparison, however, as the systems studied in this work certainly do not adhere fully to the model of an isolated complex in an inert solvent, basic to this theory [8].

4.2. Correlation functions

The dynamic phenomena responsible for the shaping of the ν_s(AH) bands are revealed by the time correlation functions, presented in Fig. 3 for TPC and Fig. 4 for TMC. As can be seen, the decay of the correlation functions is very fast, although the complexes

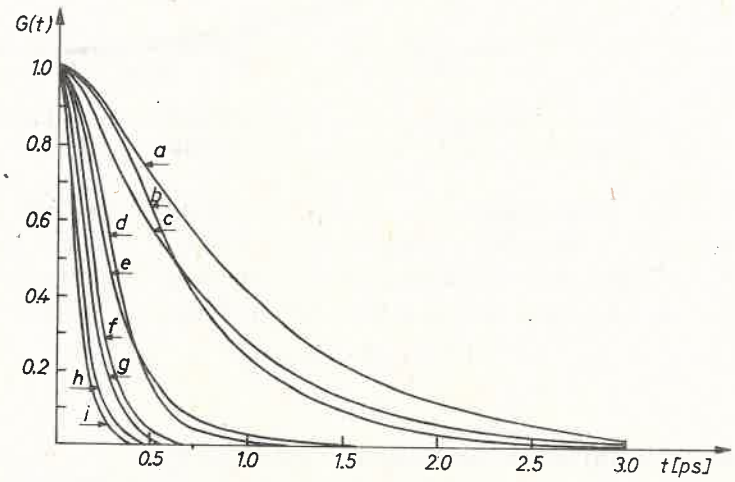

Fig. 3. Correlation functions for the ν_s(OH) vibration of Triphenylcarbinol: *a* — Heptane, *b* — Mesithylene (3613.0 cm^{-1}), *c* — Carbon Tetrachloride, *d* — Benzene, *e* — Mesithylene (3559.9 cm^{-1}), *f* — Nitromethane, *g* — Nitrobenzene, *h* — Acetonitrile, *i* — Dioxane

studied are still fairly weak. This is reflected also in the values of correlation times, collected in Table III, which diminish from 0.8–1.0 picoseconds in inert solvents to 0.1–0.2 ps for complexes with dioxane. These values are comparable in magnitude to those reported earlier for butanol and heptanol in CCl_4 (0.6 ps) and of the complex of butanol and dioxane in CCl_4 (0.1 ps) [16].

The presentation of correlation functions in semi-logarithmic scale reveals, that in every case, the plot of the logarithm of the correlation function versus time exhibits a curvature for small times, whereas for longer times it becomes distinctly linear (Fig. 5, Fig. 6). This behaviour is qualitatively well in agreement with the predictions of the theory of Ro-

bertson and Yarwood [9, 10], thus favoring the indirect relaxation mechanism in the shaping of ν_s(AH) bands. The considerable broadening of the low frequency side of bands observed in TPC complexes with nitromethane and nitrobenzene would indicate, however, that the fluctuation mechanism may be of importance in some cases.

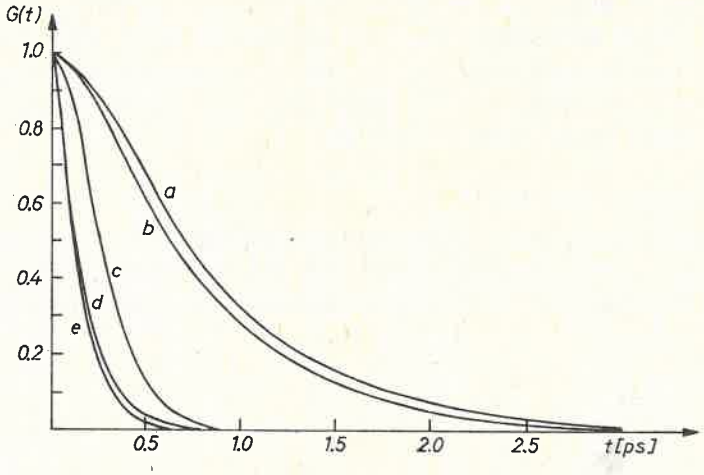

Fig. 4. Correlation functions for the ν_s(OH) vibration of Trimethylcarbinol: *a* — Carbon Tetrachloride, *b* — Heptane, *c* — Nitrobenzene, *d* — Acetonitrile, *e* — Dioxane

Another aspect of the dynamics of weak H-bonds emerges from the comparison of correlation functions of the ν_s(AH) vibration in complexes of TPC and TMC with identical acceptor molecules. As is well known, the IR correlation functions can be expressed as a product of the vibrational $G_v(t)$ and reorientational $G_{1R}(t)$ correlation functions [26]:

$$G^{IR}(t) = G_v(t)G_{1R}(t). \tag{9}$$

TABLE III

Correlation times for ν_s(OH) band of Trimethylcarbinol and Triphenylcarbinol. The values in parentheses were obtained from correlation functions calculated with respect to ν_0

Solvent	Correlation time [ps]	
	TPC	TMC
Heptane	1.09 (1.05)	0.82 (0.81)
CCl_4	0.81 (0.68)	0.90 (0.89)
Nitrobenzene	0.20 (0.18)	0.31 (0.31)
Nitromethane	0.20 (0.19)	
Benzene	0.32 (0.32)	
Mesithylene:		
3559.9 cm^{-1} band	0.32 (0.31)	
3613.0 cm^{-1} band	0.75 (0.75)	
Acetonitrile	0.15 (0.14)	0.17 (0.18)
Dioxane	0.09 (0.12)	0.17 (0.16)

Although it is known at present, that the separation of the vibrational and reorientational relaxation processes implied in Eq. (9) is not entirely correct [27, 28], Eq. (9), although only approximate, proves still very useful.

In inert solvents, where no complexes are formed, the decay of $G^{IR}(t)$ describes the time evolution of the transition dipole moment of the ν_s(OH) vibration. Thus, the reorienta-

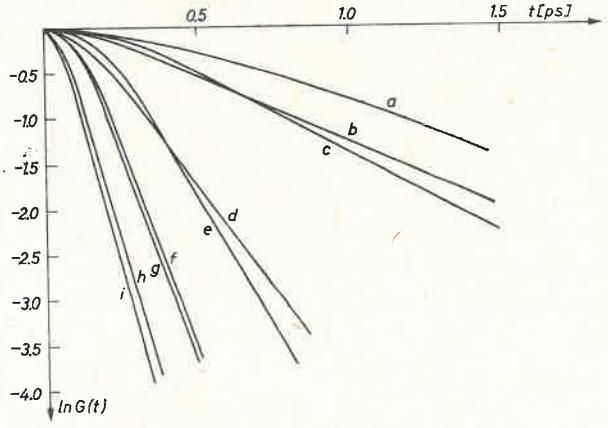

Fig. 5. Ln $G(t)$ vs t plot for the ν_s(OH) vibration of Triphenylcarbinol: a — Heptane, b — Carbon Tetrachloride, c — Mesithylene (3613.0 cm^{-1}), d — Mesithylene (3559.9 cm^{-1}), e — Benzene, f — Nitromethane, g — Nitrobenzene, h — Acetonitrile, i — Dioxane

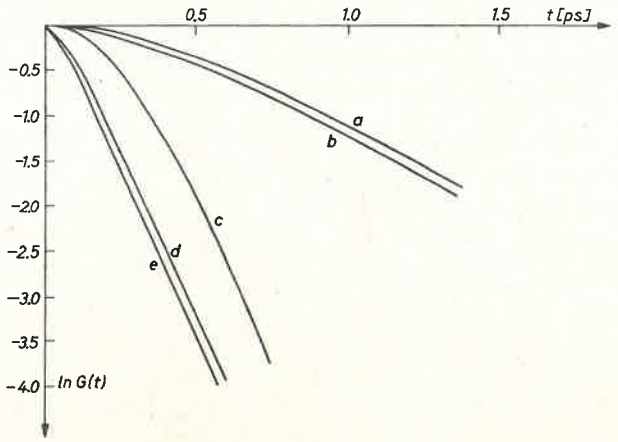

Fig. 6. Ln $G(t)$ vs t plot for the ν_s(OH) vibration of Trimethylcarbinol: a — Carbon Tetrachloride, b — Heptane, c — Nitrobenzene, d — Acetonitrile, e — Dioxane

tion of the OH group around the C–O axis can principally cause a contribution to the bandshape via $G_{1R}(t)$. In heptane the correlation functions for both TMC and TPC coincide until about 0.15 ps and at longer times the decay for TMC is faster (Fig. 7). This picture is well consistent with the findings of Dijkman [31] and suggestions of Kirchner and Richter [29] that a considerable part of the IR bandwidth of TBC in inert solvents is

caused by reorientational relaxation. At short times, the predominant shaping mechanism would be the reorientation of the OH oscillator around the C–O axis; at longer times this process is superimposed by rotational diffusion of the whole molecule, causing a faster decay for TMC than for TPC. For CCl_4 this picture is altered; in this solvent, termed "inactive", obviously the interaction between the OH group and the solvent is already sufficiently pronounced, so the vibrational term in Eq. (9) dominates, causing a faster decay of $G^{IR}(t)$ for TPC than for TMC (Fig. 8).

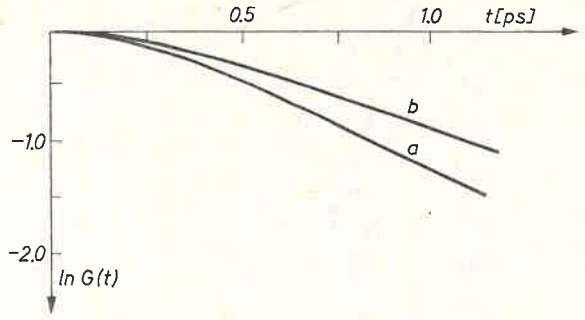

Fig. 7. Comparison of correlation functions for the ν_s(OH) band in Heptane: *a* — Trimethylcarbinol, *b* — Triphenylcarbinol

For weak R′AH···BR″ complexes the decay of $G^{IR}(t)$ for the ν_s(AH) vibration reflects the time evolution of the transition dipole moment located along the AH···B axis. Thus, rotation around this axis should not influence the shape of the band; only the tumbling of the complex around axes perpendicular to the H-bond could cause in principle a reorien-

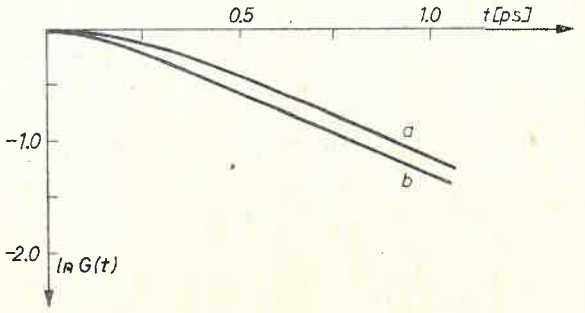

Fig. 8. Comparison of correlation functions for the ν_s(OH) band in Carbon Tetrachloride: *a* — Trimethylcarbinol, *b* — Triphenylcarbinol

tational broadening effect contributing via the decay of $G_{1R}(t)$ to the decay of $G^{IR}(t)$. If there is any contribution of this kind, it should be larger for TMC complexes than for TPC complexes; the former are less bulky, so their reorientation should be less hindered and the decay of $G_{1R}(t)$ (and consequently, also the decay of $G^{IR}(t)$) should be faster for TMC complexes, assuming $G_v(t)$ behaves equally for both donors because of the comparable

strength of H-bond in these systems. As can be seen from Figs. 9 and 10, just the opposite is observed. This can be only understood assuming, that in TPC complexes the vibrational relaxation, described by $G_v(t)$, is faster, because TPC is a slightly stronger "acid" than TMC, so the TPC complexes are slightly stronger than identical TMC complexes. It

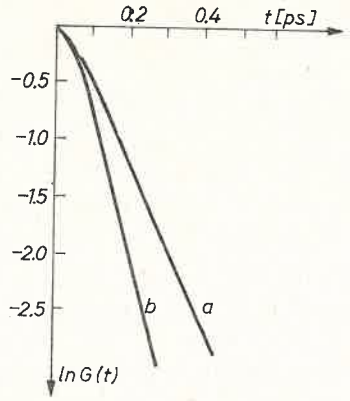

Fig. 9. Comparison of correlation functions for the ν_s(OH) vibration in Nitrobenzene: *a* — Trimethylcarbinol, *b* — Triphenylcarbinol

appears that this small difference is sufficient to offset any possible reorientational contribution. Therefore, it can be concluded, that this contribution can be safely neglected in the IR spectrum, and the shaping is due entirely to vibrational relaxation. Similar conclusions have been reached basing on other arguments [16, 17].

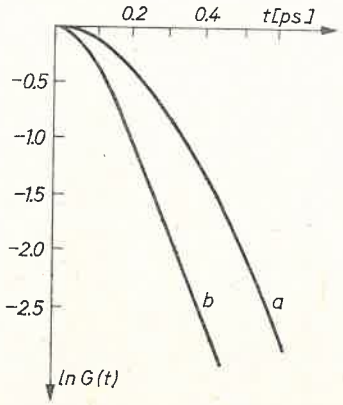

Fig. 10. Comparison of correlation functions for the ν_s(OH) vibration in Dioxane: *a* — Trimethylcarbinol, *b* — Triphenylcarbinol

The results obtained for benzene and mesitylene can serve as a good illustration of the difficulties encountered in some systems. The ν_s(OH) band in these solvents is a superposition of two bands: one corresponding to the OH···π complex, and a second, at higher wavenumbers, to the "free" OH oscillator. For mesitylene the effect is well pronounced (Fig. 11) and it was possible to separate them numerically yielding the complex band at

3559.9 cm^{-1} and the "free" band at 3613.0 cm^{-1}. During this separation, for the description of the complex band centered at 3559.9 cm^{-1} the asymmetric Cauchy–Gauss curve (1) was used, while the "free" band (3613.0 cm^{-1}) was kept symmetric, i.e. $a_2 = a_5$, $a_4 = a_6$ was set during the iteration. For benzene the "free" band is only weakly pronounced as

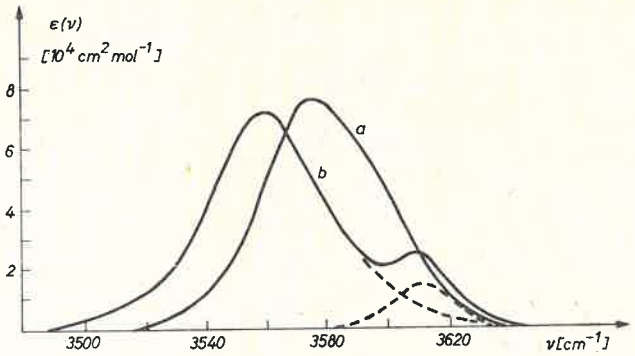

Fig. 11. Contours of the ν_s(OH) band of Triphenylcarbinol in: *a* — Benzene, *b* —•Mesithylene

an asymmetry of the high frequency side (Fig. 12). It is interesting to note that on the time scale this picture is confirmed. The correlation function of the 3559.9 cm^{-1} band resembles that of benzene, whereas the correlation function for the 3613 cm^{-1} band decays similarly as in inert solvents; the same applies to the correlation times (Table III). The point of

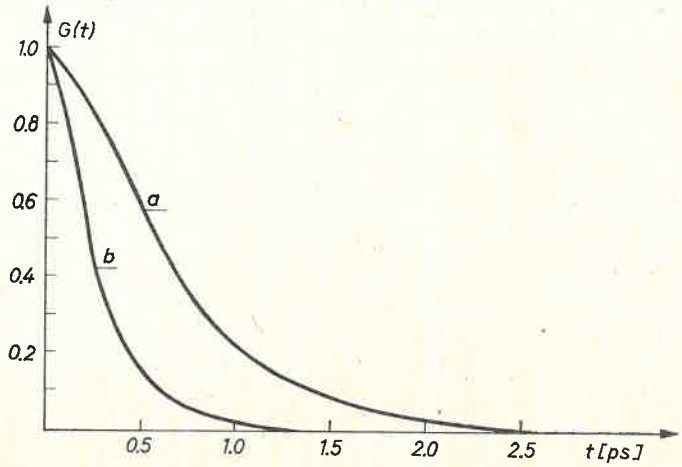

Fig. 12. Correlation functions for the ν_s(OH) band of Triphenylcarbinol in Mesithylene: *a* — 3613.0 cm^{-1} band; *b* — 3559.9 cm^{-1} band

relevance here is that hidden, unresolved bands — as in case of benzene — if not recognized and properly taken account for, will obscure the results of bandshape analysis.

In conclusion, we feel that in the light of the obtained results, as well as of earlier ones, the dominant role of the vibrational relaxation in the shaping of the IR stretching vibration bands of the proton donor group seems to be well established. Whereas for

inert solvents a reorientational contribution to the band shape cannot be excluded for the studied systems, even for very weak H-bonds the shaping is entirely due to vibrational relaxation. In the framework of the present series of experiments it is not possible to estimate the relative contributions of the indirect relaxation mechanism, which seems to be dominant, and the fluctuating field mechanism. Further experiments are in progress to clarify this important point.

We are indebted to Mr. R. Szostak for the computation of correlation functions.

REFERENCES

[1] A. Witkowski, *J. Chem. Phys.* **47**, 3645 (1967).
[2] Y. Maréchal, A. Witkowski, *Theor. Chim. Acta* **9**, 116 (1967); *J. Chem. Phys.* **48**, 3697 (1968).
[3] R. Janoschek, E. G. Weidemann, H. Pfeifer, G. Zundel, *J. Am. Chem. Soc.* **94**, 2387 (1972).
[4] R. Janoschek, E. G. Weidemann, G. Zundel, *J. Chem. Soc. Faraday Trans.* II **69**, 505 (1973).
[5] C. A. Coulson, G. N. Robertson, *Proc. R. Soc. London* **A337**, 164 (1974); **A342**, 289 (1975).
[6] H. Romanowski, L. Sobczyk, *Chem. Phys.* **19**, 361 (1977).
[7] N. Rösch, M. A. Ratner, *J. Chem. Phys.* **61**, 3344 (1974).
[8] S. Bratos, *J. Chem. Phys.* **63**, 3499 (1975).
[9] G. N. Robertson, J. Yarwood, *Chem. Phys.* **32**, 267 (1978).
[10] J. Yarwood, R. Ackroyd, G. N. Robertson, *Chem. Phys.* **32**, 283 (1978).
[11] J. De Bleijser, P. C. M. Van Woerkom, J. C. Leyte, *Chem. Phys.* **13**, 387 (1976).
[12] J. De Bleijser, P. C. M. Van Woerkom, D. Van Duijn, H. S. Kielman, J. C. Leyte, *Chem. Phys.* **13**, 403 (1976).
[13] E. Marèchal, S. Bratos, *J. Chem. Phys.* **68**, 1825 (1978).
[14] J. L. Wood, in *Spectroscopy and Structure of Molecular Complexes*, J. Yarwood, Ed., Plenum Press, London 1973, Chapter 4, p. 323.
[15] W. G. Rotschild, *Chem. Phys. Lett.* **9**, 149 (1971); *J. Chem. Phys.* **55**, 1402 (1971).
[16] R. Konopka, T. W. Żerda, Z. Gburski, A. Hacura, E. Wilk, *Chem. Phys. Lett.* **30**, 145 (1975).
[17] J. Limouzi, A. Burneau, J. P. Perchard, *Chem. Phys. Lett.* **47**, 346 (1977).
[18] W. Schindler, *Chem. Phys.* **31**, 345 (1978).
[19] K. S. Seshadri, R. N. Jones, *Spectrochim. Acta* **19A**, 1013 (1963).
[20] J. P. Hawranek, *Wiad. Chem.* **24**, 225 (1970) (in Polish).
[21] *Technique of Organic Chemistry*, A. Weisberger, Ed., Vol. VII: *Organic Solvents*, Interscience Publishers, New York 1955.
[22] J. P. Hawranek, P. Neelakantan, R. P. Young, R. N. Jones, *Spectrochim. Acta* **32A**, 85 (1976).
[23] J. P. Hawranek, *Acta Phys. Pol.* **A40**, 811 (1971).
[24] J. P. Hawranek, R. Szostak, in preparation.
[25] Z. Malarski, *Roczniki Chem.* **48**, 663, 705 (1974).
[26] S. Bratos, J. Rios, Y. Guissani, *J. Chem. Phys.* **52**, 439 (1970).
[27] P. C. M. Van Woerkom, J. de Bleijser, M. de Zwart, J. C. Leyte, *Chem. Phys.* **4**, 236 (1974).
[28] P. C. M. Van Woerkom, J. de Bleijser, M. de Zwart, J. C. Leyte, *Ber. Bunsenges. Phys. Chem.* **78**, 1303 (1974).
[29] H. H. Kirchner, W. Richter, *Ber. Bunsenges. Phys. Chem.* **81**, 1250 (1977).
[30] E. T. G. Lutz, J. H. Van Der Maas, *Spectrochim. Acta* **34A**, 915 (1978).
[31] F. G. Dijkman, *Mol. Phys.* **36**, 705 (1978).